Evaluation of the protective effects of sarains on H_2O_2-induced mitochondrial dysfunction and oxidative stress in SH-SY5Y neuroblastoma cells

Rebeca Alvariño[a], Eva Alonso[a], Marie-Aude Tribalat[b], Sandra Gegunde[a], Olivier P. Thomas [c], Luis M. Botana[a*]

[a] Departamento de Farmacología, Facultad de Veterinaria, Universidad de Santiago de Compostela, Lugo 27003, Spain

[b] Géoazur UMR Université Nice Sophia Antipolis, 250 Avenue Albert Einstein, 06108 Nice, France

[c] National University of Ireland Galway, Marine Biodiscovery, School of Chemistry, University Road, Galway, Ireland

*Email: luis.botana@usc.es. Phone/Fax: +34982822233.

Abstract

Sarains are diamide alkaloids isolated from the Mediterranean sponge *Haliclona (Rhizoniera) sarai* that have previously shown antibacterial, insecticidal and anti-fouling activities. In this study, we examined for first time the neuroprotective effects of sarains 1, 2 and A against oxidative stress in a human neuronal model. SH-SY5Y cells were co-incubated with sarains at concentrations ranging from 0.01 to 10 µM and the well-known oxidant hydrogen peroxide at 150 µM for 6 hours and the protective effects of the compounds were evaluated. Among the sarains tested, sarain A was the most promising compound, improving mitochondrial function and decreasing reactive oxygen species levels in human neuroblastoma cells treated with the compound at 0.01, 0.1 and 1 µM. This compound was also able to increase the activity of the antioxidant enzymes superoxide dismutases by inducing the translocation of the nuclear factor E2-related factor 2 (Nrf2) to the nucleus at the lower concentrations tested (0.01 and 0.1 µM). Moreover, sarain A at 0.1 and 1 µM blocked the mitochondrial permeability transition pore (mPTP) opening through cyclophilin D inhibition. These results suggest that the protective effects produced by the treatment with sarain A are related with its ability to block the mPTP and to enhance the Nrf2 pathway, indicating that sarain A may be a candidate compound for further studies in neurodegenerative diseases.

Keywords: sarains, oxidative stress, Nrf2, mPTP, cyclophilin D, neuroprotection

Acknowledgments

The research leading to these results has received funding from the following FEDER cofunded-grants. From CDTI and Technological Funds, supported by Ministerio de Economía, Industria y Competitividad, AGL2014-58210-R, AGL2016-78728-R (AEI/FEDER, UE), ISCIII/PI16/01830 and RTC-2016-5507-2. From CDTI under ISIP Programme, Spain, IDI-20130304 APTAFOOD and ITC-20161072. From the European Union's Seventh Framework Programme managed by REA – Research Executive Agency (FP7/2007-2013) under grant agreement 312184 PHARMASEA.

1. Introduction

Mitochondria are the main source of reactive oxygen species (ROS) in the cell. These organelles produce ROS through oxidative phosphorylation like hydrogen peroxide (H_2O_2), superoxide ($O_2^{\cdot-}$), and hydroxyl radical ($OH^{\cdot}$). Under physiological conditions, these oxygen species exert biological functions (Weidinger and Kozlov 2015) and their levels are tightly regulated by antioxidant molecules like glutathione (GSH), and enzymes like superoxide dismutases (SODs), catalase (CAT) and glutathione peroxidase (GPx). Under conditions of oxidative stress, the balance between ROS production and the antioxidant systems is displaced, resulting in significant cell damage. Oxidative stress has been associated with neurodegenerative disorders like Alzheimer´s Disease (AD), Parkinson´s Disease (PD), Amytrophic Lateral Sclerosis (ALS) or Huntington's Disease (Lin and Beal 2006). This association is partly caused by the susceptibility of the brain to oxidative damage due to its high rate of energy consumption, relative low levels of antioxidant defences and high concentrations of polyunsaturated fatty acids. ROS contribute to neurodegeneration causing damage to proteins, DNA and RNA, lipid peroxidation as well as leading to changes in cell function and potentially cell death (Gandhi and Abramov 2012).

The reduction of ROS levels through the enhancement of antioxidant systems is a good therapeutic approach to alleviating these pathologies. In this sense, the nuclear factor E2-related factor 2 (Nrf2)-antioxidant response element (ARE) pathway has been proposed as a potential target against

neurodegeneration (Lu et al. 2016; McBean et al. 2016). Nrf2 is a primary sensor of oxidative stress and regulates the expression of several genes implicated in antioxidant systems like SODs, CAT, GPx and glutathione reductase (Malhotra et al. 2010). In neurodegenerative diseases the Nrf2 pathway is impaired. Nrf2 levels are reduced in AD brains, and Nrf2 activation in nigral neurons is not enough to protect the cells from oxidative stress in PD (Ramsey et al. 2007). Nrf2 cytoplasmic repression is regulated by Kelch-like ECH-associated protein 1 (Keap1), which binds the transcription factor via an association with Cullin 3-based E3 ubiquitin ligase, controlling Nrf2 proteasomal degradation. Keap1 is sensitive to small molecules, called inducers, which can disrupt the binding with Nrf2. Then, the factor translocates to the nucleus where it forms a heterodimer with small Maf proteins and binds to the ARE, inducing the expression of detoxifying genes (Magesh et al. 2012). Recently, Nrf2 activation has been also related to the mitochondrial function through the regulation of other pathways, as the oxidative phosphorylation, the glycolysis or the lipid metabolism (Esteras et al. 2016).

Moreover, the increase in ROS levels observed in neurodegenerative diseases can produce the opening of the mitochondrial permeability transition pore (mPTP) (Rao et al. 2014). The pore is a non-selective channel that allows solutes with molecular weights less than 1500 Da to cross from the mitochondrial matrix to the cytosol. The main components of the mPTP are the voltage-dependent anion channel in the outer mitochondrial membrane, the adenine nucleotide translocator (ANT) in the inner membrane and cyclophilin D (CypD), located in the mitochondrial matrix. When the levels of ROS increase, CypD binds to the ANT in the inner mitochondrial membrane and triggers the opening of the mPTP. The massive formation of the channel produces the dissipation of the proton motive force, the depletion of ATP, and the release of apoptogenic factors to the cytosol, producing cell death(Du and Yan 2010). It has been demonstrated that the translocation of CypD to the inner mitochondrial membrane is an essential step for the initiation of the mPTP. Low levels of CypD are correlated with a decreased sensitivity to mPTP formation in brain mitochondria (Eliseev et al. 2007) and its genetic ablation prevents from mPTP opening (Baines et al. 2005). The mitochondrial dysfunctions observed in AD, PD and ALS have been related with mPTP. Particularly, CypD levels are increased in AD brains, increasing the risk of mPTP formation. In fact, the genetic deficiency of this component has improved memory in

a murine model of AD (Du et al. 2008). For these reasons, the blockage of the mPTP through CypD inhibition is a potential therapeutic tool in the treatment of neurodegenerative disorders.

Some marine natural compounds have been shown to be drug candidates in neurodegenerative diseases (Grosso et al. 2014). Particularly, sponge-derived compounds have exhibited beneficial effects against oxidative stress (Sasaki et al. 2011) and neurodegenerative diseases (Leirós et al. 2015). Alkaloids produced by the Mediterranean sponge *Haliclona (Rhizoniera) sarai* and named sarains have already shown antibacterial activity, insecticidal effects and anti-fouling properties (Blihoghe et al. 2011; Caprioli et al. 1992; Defant et al. 2011). Sarains also induce erythrocyte lysis and acetylcholinesterase inhibition (Defant et al. 2011), but their antioxidant capacity has not been tested so far. Human neuroblastoma SH-SY5Y cells have been widely used as a cell model system for studying oxidative stress (Huang et al. 2014). In this work, we examined for first time the cytoprotective effect of sarains 1, 2 and A against H_2O_2-induced oxidative stress in human neuroblastoma cells.

2. Materials and Methods

2.1. Chemicals and solutions

Tetramethylrhodamine methyl ester (TMRM), Thiol Tracker™Violet, MitoProbe™ Transition Pore Assay Kit and 5-(and-6)-carboxy-2′,7′-dichlorodihydrofluorescein diacetate (carboxy-H_2DCFDA) were purchased from Thermo Fisher Scientific (Waltham, MA, USA). Other chemical were reagent grade and purchased from Sigma-Aldrich (Madrid, Spain).

2.2. Isolation and purification

^{1}H and ^{13}C NMR spectra were recorded on a 500 MHz Bruker Avance NMR spectrometer. Chemical shifts (δ) are recorded in ppm with CD_3OD (δ_H 3.31 ppm and δ_C 49.00 ppm) as internal reference. HRMS data were obtained from a UHPLC-QqToF (Bruker Impact II). HPLC purifications were carried out on a Waters 600 system equipped with a Waters 717 plus Autosampler, a Waters 996 photodiode array detector, and a Sedex 55 evaporative light-scattering detector (SEDERE, France), and on a Jasco PU 2087 Plus system equipped with a single wavelength UV detector UV 2075 Plus and a Sedex 85

106 evaporative light-scattering detector (SEDERE, France). Detection wavelengths were set at 210, 238
107 and 267 nm.

108 *2.2.1 Animal material*

109 One specimen of *Haliclona* (*Rhizoniera*) *sarai* was collected in March 2013 by SCUBA diving at Saint-
110 Jean-Cap-Ferrat (43° 41' 29.9646'', 7° 19' 11.8668''), at depth of 25 m, and kept frozen until used.

111 *2.2.2. Extraction and isolation*

112 The sample of *Haliclona* (*Rhizoniera*) *sarai* was freeze-dried and then ground to obtain a dry powder
113 (4.1 g) which was exhaustively extracted with MeOH (3 × 100 mL) to yield 2.1 g of crude extract after
114 concentration under reduced pressure. The crude extract was fractionated by Reverse Phase Vacuum
115 Liquid Chromatography over RP-18 silica gel (200 g) with a step gradient of H_2O (F1 fraction, 920 mg),
116 MeOH/H_2O 2:1 v/v (F2 fraction, 260 mg), MeOH/H_2O 3:1 v/v (F3 fraction, 56 mg), MeOH (F4 fraction,
117 54 mg) and DCM (F5 fraction, 94 mg) (500 mL each). Fractions F4 (54 mg, 30 mg.mL^{-1}) and F5 (94
118 mg, 30 mg.mL^{-1}) fractions were combined and then subjected to semi-preparative HPLC purification
119 (Waters system, Phenomenex Gemini C6-phenyl column 250 mm × 10 mm, 5 µm) eluted with a gradient
120 of H_2O/CH_3CN/TFA: isocratic step from 0 min to 5 min (70:30:0.1), then a first gradient step from 5
121 min to 15 min (70:30:0.1 to 10:90:0.1) and a second gradient from 15 min to 20 min (90:10:0.1 to
122 0:100:0.1) (flow rate 3.0 mL.min^{-1}, injection volume: 70 µL) to give 16 fractions labeled F4F5P1-16.
123 Those first steps of purification led to pure compounds (≥95%): sarain 2 (25 mg, F4F5P5) and sarain 1
124 (24 mg, F4F5P6). F4F5P1 was purified (Jasco system, Waters Symmetry Prep, 300 mm × 7.8 mm, 7
125 µm) according to the following gradient of H_2O/CH_3CN/TFA: isocratic step from 0 min to 5 min
126 (80:20:0.1), then a gradient step from 5 min to 15 min (80:20:0.1 to 60:40:0.1) and finally an isocratic
127 step from 15 min to 20 min (60:40:0.1), leading to sarain A (15 mg; purity ≥95%). Comparison of NMR
128 and MS data with the literature confirmed the structure of these known compounds (Cimino et al. 1989;
129 Cimino et al. 1986).

130 *2.3. Cell culture*

Human neuroblastoma SH-SY5Y cell line was purchased from American Type Culture Collection (ATCC), number CRL2266. The cells were maintained in Dulbecco´s Modified Eagle´s medium: Nutrient Mix F-12 (DMEM/F-12) supplemented with 10% fetal bovine serum (FBS), glutamax, 100 U/mL penicillin and 100 µg/mL streptomycin at 37 C in a humidified atmosphere of 5% CO_2 and 95% air. Cells were dissociated weekly using 0.05% trypsin/EDTA. All reagents were provided by Thermo Fisher Scientific (Waltham, MA, USA).

2.4. Cell viability and mitochondrial function assays

One day prior to experiments, cells were seeded in 96-well plates at a density of $3x10^4$ cells per well. SH-SY5Y cells were treated with sarains at different concentrations (0.01, 0.1, 1, and 10 µM) for 24 h. Lactate dehydrogenase (LDH) release was used as an indicator of cell survival. The LDH Assay kit (Abcam, Cambridge, UK) was used for measuring its activity, following the commercial protocol.
The effect of compounds on mitochondrial function was evaluated by MTT (3-(4, 5-dimethyl thiazol-2-yl)-2,5-diphenyl tetrazolium bromide) assay (Mosmann 1983; Vega-Avila and Pugsley 2011). This probe has been widely used to evaluate mitochondrial function in SH-SY5Y cells (Coccini et al. 2014; Park et al. 2014; Tricarico et al. 2016) and in other cell lines (Blanquer-Rossello et al. 2017; Chakraborty et al. 2016; Kharroubi et al. 2017). SH-SY5Y cells were rinsed with saline solution and 200 µL of MTT (500 µg/mL) dissolved in saline buffer were added to each well. Following 1 h of incubation at 37 C, SH-SY5Y cells were disaggregated with 5% sodium dodecyl sulphate. Absorbance of formazan crystals was measured at 595 nm with a spectrophotometer plate reader. Saponin from quillaja bark was used as death control and its absorbance was subtracted from the other data.

2.5. Neuroprotection and mitochondrial membrane potential assays

The ability of compounds to protect cells from H_2O_2 damage was also evaluated with MTT probe. Cells were co-treated with sarains 1, 2 and A at non-toxic concentrations (0.01, 0.1, 1, and 10 µM) and 150 µM H_2O_2 for 6 h and the assay was carried out as described above. All experiments were performed at least three times.

156 The mitochondrial membrane potential ($\Delta\Psi_m$) was assessed using the TMRM probe. SH-SY5Y cells
157 were seeded in 96-well plates at a density of $3x10^4$ cells per well and allowed to attach for 24 h. After
158 this time, cells were treated with 150 μM H_2O_2 and sarains 1, 2 and A at different concentrations (0.01,
159 0.1, 1, and 10 μM) for 6 h.
160 Cells were washed twice with saline solution and 1 μM TMRM was added to each well for 30 min at
161 37 C. After incubation, cells were solubilized with DMSO and H_2O at 50% and the fluorescence was
162 monitored with a spectrophotometer plate reader (535 nm excitation and 590 nm emission). All
163 experiments were performed at least three times.

164 The endogenous antioxidant vitamin E (vitE) at 25 μM was used to validate the *in vitro* model in all the
165 assays.

166 *2.6. Determination of intracellular reactive oxygen species levels*

167 Intracellular levels of ROS were determined with carboxy-H_2DCFDA (5-(and-6)-carboxy-2′,7′-
168 dichlorodihydrofluorescein diacetate) as previously described (Ouazia et al. 2014) with modifications.
169 SH-SY5Y cells were seeded one day before the experiments in 96-well plates at a density of $3x10^4$ cells
170 per well. Cells were co-treated with compounds at various concentrations (0.01, 0.1, 1, and 10 μM) and
171 150 μM H_2O_2 for 6 h. 25 μM vitE was used as positive control. Following treatment with compounds
172 and H_2O_2, SH-SY5Y cells were washed twice with serum-free medium. Then, 20 μM carboxy-
173 H_2DCFDA dissolved in serum-free medium was added to the cells. After 1 h at 37 C, the medium
174 containing the fluorescence dye was replaced with PBS. The plate was incubated for 30 min at 37 C and
175 fluorescence was read at 527 nm, with an excitation wavelength of 495 nm. All experiments were
176 performed at least three times.

177 *2.7. Glutathione assay*

178 GSH levels were determined using Thiol Tracker™ Violet dye, which reacts with reduced thiols in cells.
179 Reduced GSH represents the majority of intracellular free thiols, so this probe can be used to estimate
180 its levels in cells. Measurements were performed following manufacturer´s instructions. One day before
181 the experiments, SH-SY5Y cells were seeded in 96-well plates at $3x10^4$ cells per well. Then, cells were

182 treated with 150 μM H_2O_2 and sarains 1, 2 and A at 0.01, 0.1, 1 and 10 μM for 6 h. After this time, cells
183 were washed twice with PBS and loaded with 100 μL of prewarmed ThiolTracker™ Violet dye (10 μM)
184 for 30 min at 37 C. The fluorescence was measured at 404 nm excitation and emission at 526 nm. All
185 experiments were performed at least three times. 25 μM vitE was used to test the validity of the *in vitro*
186 model.

187 *2.8. Catalase and superoxide dismutases activity assays*

188 CAT activity was measured with Amplex® Red Catalase Assay Kit (Thermo Fisher Scientific,
189 Waltham, MA, USA). SH-SY5Y neuroblastoma cells were seeded at $1x10^5$ cells per well. Cells were
190 co-treated with sarains (0.01, 0.1, 1, and 10 μM) and 150 μM H_2O_2 for 6 h. Cell lysates were processed
191 following manufacturer's protocol and fluorescence was read at 530 nm excitation and 590 nm emission.
192 Enzymatic activity was calculated by subtracting sample values to the no-CAT control.

193 SODs activity was assessed with SOD determination Kit (Sigma-Aldrich, Madrid, Spain). Cells were
194 seeded in 6-well plates at a density of $1x10^6$ cells per well and incubated with compounds (0.01, 0.1, 1
195 and 10 μM) and 250 μM H_2O_2 for 24 h. Then, SH-SY5Y cells were rinsed with ice-cold PBS and 100
196 μL of lysis buffer (0.1 M Tris- HCl, pH 7.4 containing 0.5% Triton X-100, 5 mM β-mercaptoethanol
197 and 0.1 mg/mL PMSF) were added to each well. Cell lysates were centrifuged at 14000 g for 5 min at
198 4°C and SODs assay was performed following manufacturer's protocol. The absorbance was read at
199 450 nm and the SODs activity was determined by subtracting the sample values to the no-SODs blank.

200 *2.9. Western blot and immunocytochemistry analysis*

201 For western blot analysis, SH-SY5Y cells were seeded in 6-well plates at $4x10^5$cells per well and treated
202 with sarain A at 0.01, 0.1, 1, and 10 μM for 6 h. After treatment with the compound, neuroblastoma
203 cells were rinsed twice with ice-cold PBS. Next, 100 μL of an ice-cold hypotonic solution buffer (20
204 mM Tris-HCl pH 7.4, 10 mM NaCl and 3 mM $MgCl_2$, containing a complete phosphatase/protease
205 inhibitors cocktail from Roche) were added. Cells were scrapped, incubated on ice for 15 min and finally
206 centrifuged at 3000 rpm, 4 C during 10 min. The supernatant was collected as the cytosolic fraction and
207 the pellet was resuspended in an ice-cold nuclear extraction buffer(100 mM Tris pH 7.4, 2 mM Na_3VO_4,

100 mMNaCl, 1% Triton X-100, 1 mM EDTA, 10% glycerol, 1 mM EGTA, 0.1% SDS, 1 mM NaF, 0.5% deoxycholate, and 20 mM $Na_4P_2O_7$, containing 1 mM PMSF and a protease inhibitor cocktail). Samples were incubated for 30 min, vortexing in 10 min intervals, and centrifuged at 14000 g and 4°C for 30 min. The supernatant was saved for nuclear protein fraction. This fraction was quantified by Bradford method, whereas cytosolic protein fraction was quantified using Direct Detect system (Millipore, Darmstadt, Germany). Samples containing 20 µg (cytosolic fraction) or 10 µg (nuclear fraction) were used for electrophoresis, which was resolved in a 10% sodium dodecyl sulphate polyacrylamide gel (Biorad, Hercules, CA, USA) and transferred onto PVDF membranes(Millipore). Snap i.d protein detection system was used for membrane blocking and antibody incubation. Anti-NF-E2 related factor 2 antibody was used to detect Nrf2 (1:1000, Millipore), and signal was normalized using β-actin (1:10000, Millipore) for cytosolic fraction and laminB1 (1:1000, Abcam) for nuclear fraction. Protein bands were detected using Supersignal West Pico Luminiscent Substrate and Supersignal West Femto Maximum Sensitivity Substrate (Thermo Fisher Scientific) and Diversity GeneSnap system (Syngene, Cambridge, U.K.) and software.

For immunocytochemistry determination, SH-SY5Y cells were seeded in 12-well plates at a density of $2x10^5$ cells/well and treated with sarain A (0.01 µM) during 6 h. Cells were fixed with 4% paraformaldehyde and after washed three times with PBS. Blocking buffer (5% BSA, 0.1% Triton x-100) was added to each well for 2 h at room temperature. Then, SH-SY5Y cells were incubated with anti-NF-E2 related factor 2 (1:200, Millipore) primary antibody overnight at 4°C. After this time, cells were incubated with Cy3 goat anti-rabbit (1:1000, Thermo Fisher Scientific) during 2 h at room temperature. Hoechst 33258 (Thermo Fisher Scientific) at 1 µg/µL was used for nuclear staining. Fluorescent measurements were done in a Nikon Eclipse TE2000-E inverted microscope attached to the C1 laser confocal system and EZ-C1 V.2.20 software (Nikon Instruments Europe B.V., Amstelveen, Netherlands) by using the 408 and 561 nm lasers for excitation and 515 and 650 nm emission filters. The images were collected using 40 x oil immersion objective (Nikon).

2.10. Measurement of ATP content

SH-SY5Y cells were seeded at 5x 10^4 cells per well and incubated with sarain A (0.01, 0.1, 1 and 10 μM) and 150 μM H_2O_2 for 6 h. The levels of ATP were assessed with the Luminescent ATP Detection Assay Kit (Abcam, Cambridge, UK), following the manufacturer's protocol (Pertega-Gomes et al. 2015; Zhou et al. 2016).

2.11. Mitochondrial membrane permeability transition pore measurement

The blockage of mPTP by sarains 1, 2 and A was determined with the MitoProbe™ Transition Pore Assay Kit (Nguyen et al. 2011; Petronilli et al. 1999) following manufacturer's instructions. Briefly, SH-SY5Y human neuroblastoma cells were resuspended in prewarmed PBS/Ca^{+2} buffer at a final concentration of 1x10^6 cells/mL. Cells were loaded with 0.01 μM Calcein-AM and incubated at 37 C for 15 min. Then, 0.4 mM $CoCl_2$ and compounds at different concentrations (0.01, 0.1 and 1μM) were added and incubated for 15 min at 37 C. CsA at 0.2 μM was used as positive control. After this incubation, cells were centrifuged and resuspended in 100 μL of PBS. Just before analysing, 1 mM *tert*-Butyl hydroperoxide (TBHP) was added to the samples to induce the pore opening. Fluorescence intensity was measured at 488 nm excitation and 517 nm emission wavelengths by flow cytometry using the ImageStream MKII (Amnis Corporation, Merck-Millipore).The fluorescence of 10000 events was analysed with IDEAS Application vs 6.0 (Amnis Corporation, Merck-Millipore).

2.12. Cyclophilin D enzyme inhibition assay

The inhibition of the peptidyl-prolyl *cis-trans* isomerase (PPIase) activity of CypD by sarain A was determined by following the rate of hydrolysis of *N*-succinyl-Ala-Ala-Pro-Phe-*p*-nitroanilide by chymotrypsin. CsA was used as positive control. The assay was performed as previously described (Yan et al. 2015) with small modifications. The assay buffer (20 mM Tris-HCl, 50 mM NaCl, pH 7.8) with CypD (1 nM) and the compounds at concentrations ranging from 0.001 to 10 μM were precooled at 4 C for 1h. After that time, chymotrypsin at 0.4 mg/mL in 1 mM HCl was added to each well. The reaction was started by the addition of the peptide (0.1 mg/mL in 500 mM LiCl in tetrahydrofuran). The absorbance at 380 nm was monitored with a spectrophotometer plate reader. The blank rates of hydrolysis (in absence of CypD) were subtracted from the rates in the presence of the enzyme. The half-

maximal inhibitory concentration (IC_{50}) was calculated by fitting the data with a log(inhibitor) *vs*. response model of GraphPad Prism 5.0 software.

2.13. Statistical Analyses

Data are presented as mean ± SEM. Differences were evaluated by Student´s *t*-tests and statistical significance was considered at $p < 0.05$.

3. Results

3.1. Protective effect of sarains 1, 2 and A on H_2O_2-treated SH-SY5Y cells

Firstly, SH-SY5Y cells were treated with different concentrations of sarains 1, 2 and A (Fig. 1) (0.01, 0.1, 1 and 10 µM) for 24 h to assess the compounds safety. Cell viability was determined by monitoring LDH release to the medium. None of the compounds showed cytotoxic effects at these concentrations (Fig. 2a).

The effect of sarains on mitochondrial function was evaluated by MTT assay. Human neuroblastoma cells were treated with compounds at 0.01, 0.1, 1 and 10 µM for 24 h. Neither sarains 1, 2 nor sarain A displayed toxic effects on mitochondria (Fig. 2b), confirming the LDH results. On the other hand, the treatment with sarain 2 at 0.1 and 1 µM significantly increased the mitochondrial function in SH-SY5Y cells.

H_2O_2 is a common oxidant, which has been shown to induce oxidative stress in SH-SY5Y human neuroblastoma cells (Zhang et al. 2012). Cells were co-treated with sarains at different concentrations (0.01, 0.1, 1, and 10 µM) and 150 µM H_2O_2 for 6 h and the protective effect of the compounds was evaluated by MTT (Fig. 3). A decrease in mitochondrial function of 29.3 ± 2.23% ($p<0.001$) was observed in cells treated with 150 µM H_2O_2 alone with respect to untreated cells. In the MTT assay, vitE protected cells against H_2O_2 damage, increasing mitochondrial function up to untreated cells levels (118.9± 13.0%, $p<0.001$). Sarains 1 and 2 showed no protective effects on cells, whereas sarain A at 0.01, 0.1 and 1 µM significantly improved the mitochondrial function loss induced by H_2O_2 (99.05 ± 13.6%, $p<0.05$; 87.0 ± 8.3%, $p<0.05$ and 89.7 ± 7.9%, $p<0.05$, respectively). However, this compound at 10 µM, together with 150 µM H_2O_2, produced a decrease in the mitochondrial function (39.2 ±8.9%).

In order to better understand the effects of sarains on mitochondria, the $\Delta\Psi_m$ was assessed by TMRM assay. TMRM is a fluorescent lipophilic cationic dye that accumulates within mitochondria in inverse proportion to $\Delta\Psi_m$, that is, hyperpolarized mitochondria will accumulate more dye than depolarized mitochondria. Cells were treated with the compounds at four concentrations (0.01, 0.1, 1, and 10 μM) and 150 μM H_2O_2 for 6 h. SH-SY5Y cells treated only with H_2O_2 presented a decrease in $\Delta\Psi_m$ of 17.1 ± 1.8% (p<0.001) *versus* control cells. Fig. 4a shows that sarain 1 had no effect on the restoration of the mitochondrial membrane potential against H_2O_2 damage, and sarain 2 only had effect at the highest concentration tested (10 μM), with an increase of 122.2 ±4.5% (p<0.05). Sarain A exhibited a dose-dependent response, resulting in total recovery of the $\Delta\Psi_m$ at the four concentrations tested (0.01, 0.1, 1 and 10 μM), reaching 100.1 ± 5.3% (p<0.01), 102.8 ± 3.8% (p<0.01), 111.7 ± 7.4% (p<0.05) and 140.9 ± 2.5% (p<0.01) respectively, compared to cells treated only with 150 μM H_2O_2. These percentages are similar to the levels reached by cells co-treated with 25 μM vitE (103.8 ± 6.2%, p<0.05).

To determine if the compounds of *Haliclona* (*Rhizoniera*) *sarai* were diminishing ROS release, carboxy-H_2DCFDA was used to monitor the levels of ROS in neuroblastoma cells co-treated with sarains 1, 2, A and H_2O_2 as described above. Carboxy-H_2DCFDA is converted by cellular esterases to carboxy-H_2DCFH, non-fluorescent, that can react with ROS and be oxidized to carboxy-H_2DCF, fluorescent (Halliwell and Whiteman 2004). So, increasing fluorescence will indicate an increment in ROS production. The treatment with H_2O_2 alone produced an increase of 28.8 ± 3.2% (p<0.001) in ROS levels with respect to untreated cells (Fig.4b). Co-incubation with sarain 1 at 0.01 and 1 μM significantly reduced ROS levels to 94.9 ± 9.3% (p<0.05) and 107.4 ± 5.5% (p<0.05), respectively. Sarain 2 only had effect at the highest concentration (10 μM), diminishing ROS to 110.8 ± 1.5% (p<0.05). Sarain A was again the most efficient compound, decreasing ROS levels at 0.01 (103.4 ± 1.7%; p<0.05), 0.1 (112.7 ±3.0%; p<0.05) and 1 μM (106.3 ± 6.8%; p<0.05), the same concentrations that exhibited protective effects on MTT assay. The treatment with 25 μM vitE also diminished ROS levels until 104.4 ± 6.1% (p<0.01).

3.2. Effect of sarains on the antioxidant systems of SH-SY5Y cells

312 The ability of sarains 1, 2 and A to enhance the antioxidant defences of SH-SY5Y cells was also
313 evaluated by determining the levels of GSH and the activities of antioxidant enzymes (CAT and SODs).
314 GSH is the main non-enzymatic antioxidant in cells and plays an important role in reducing oxidative
315 stress. In order to assess the effect of sarains on GSH content, its level was measured using Thiol Tracker
316 Violet dye. The cells treated with H_2O_2 presented a significant decrease in GSH content, 18.5± 1.0%
317 (p<0.001) *versus* control cells. Neither sarains 1, 2 nor sarain A increased GSH levels in cells co-treated
318 with compounds and 150 μM H_2O_2 for 6 h (Fig. 5). The enzyme CAT is responsible of the conversion
319 of H_2O_2 to water, its activity in SH-SY5Y cells treated with 150 μM H_2O_2 was significantly decreased
320 until 78.8± 11.13 % (p<0.01) compared to untreated cells. The addition of sarains 1, 2 and A was not
321 able to increase the activity of the enzyme (Fig. 6a). Finally, SODs are the major antioxidant enzymes,
322 specialized in scavenging $O_2^{\cdot-}$.We determined the effect of sarains on SODs activity by monitoring the
323 inhibition in the formation of WST-1 formazan, which is linearly related to the activity of these enzymes.
324 The treatment with 250 μM H_2O_2 for 24 h produced a decrease in SODs activity of 26.2± 0.8% (p<0.001)
325 with respect to control cells (Fig. 6b). The addition of sarains 1 and 2 to the cells showed no effect on
326 the decrease of SODs activity produced by H_2O_2. The treatment with sarain A significantly improved
327 the activity of SODs at all the concentrations tested (0.01, 0.1, 1 and 10 μM), with percentages of 85.6±
328 4.0 % (p<0.05), 82.8± 3.5% (p<0.05), 89.4± 2.1% (p<0.01), 87.7± 3.11% (p<0.05), respectively.

329 *3.3. Induction of Nrf2-ARE pathway by sarain A*

330 Nrf2 translocation to the nucleus induces the expression of several genes implicated in antioxidant
331 defences. Moreover, Nrf2 has been recently implicated in the availability of substrates for oxidative
332 phosphorylation (Holmstrom et al. 2013) and in the regulation of mitochondrial biogenesis (Itoh et al.
333 2015).
334 In view of the protective effects produced by sarain A against H_2O_2 damage and its capacity to increase
335 SODs activity, this compound was chosen to test its ability to induce Nrf2 translocation.
336 In order to evaluate the capacity of the compound to produce Nrf2 translocation to the nucleus,
337 neuroblastoma cells were treated with sarain A at 0.01, 0.1, 1 and 10 μM for 6 h. Cells were lysed and
338 Nrf2 expression was analysed by western blot in nuclear and cytosolic fractions. Results are expressed

339 in percentage of untreated cells (Fig. 7a, b). Nrf2 expression in the nucleus (Fig. 7a) was significantly
340 increased by the treatment with sarain A at 0.01 (194.5± 23.9%, $p<0.05$) and 0.1 μM (133.2± 9.5%,
341 $p<0.05$), whereas Nrf2 cytosolic levels showed no significant variations with respect to control (Fig.
342 7b). To confirm the results obtained by western blot, cells were treated with the compound at the most
343 effective concentration (0.01 μM) for 6 h and immunocytochemistry analysis was performed. The
344 immunofluorescence evaluation of Nrf2 agreed with western blot results, SH-SY5Y cells treated with
345 sarain A showed an increase in the expression of Nrf2 in the nucleus with respect to untreated cells (Fig.
346 7c). These results confirm that sarain A is able to improve the mitochondrial function and to activate the
347 antioxidant machinery by promoting Nrf2 translocation to the nucleus.

348 *3.4. Effect of sarain A on ATP levels*

349 In neurodegenerative diseases, ATP production is impaired through many mechanisms as alterations in
350 the complexes of the electronic transport chain, in glycolysis, or in TCA cycle (Burchell et al. 2010;
351 Cardoso et al. 2016). It has been shown that Nrf2 activation enhances ATP production by increasing the
352 availability of substrates for respiration (Holmstrom et al. 2013). Due to the ability of sarain A to activate
353 Nrf2, we evaluated if the compound was able to improve the production of ATP. The levels of ATP
354 were assessed after the co-treatment with sarain A and 150 μM H_2O_2 for 6 h. SH-SY5Y cells treated
355 with H_2O_2 alone presented a decrease in ATP levels until a 48.6± 11.4 % ($p<0.01$) *versus* untreated cells
356 (Fig. 7d). The treatment with sarain A significantly recovered the levels of ATP at 0.01μM (91.4± 6.3%,
357 $p<0.05$) compared with cells treated with H_2O_2 alone. ATP levels were also augmented when
358 neuroblastoma cells were treated with sarain A at 0.1 and 1 μM, although this increase was not
359 statistically significant.

360 *3.5. Blockage of mPTP by sarain A through CypD inhibition*

361 As the opening of the mPTP is one of the causes of the impairment in mitochondrial function observed
362 in neurodegeneration (Corona and Duchen 2015), we tested if these compounds could be also
363 modulating the pore opening. The ability of sarains to block mPTP opening was evaluated by flow
364 cytometry using the MitoProbe Transition Pore Assay Kit. Cells were loaded with calcein-AM, which

accumulates in cytosol and cell compartments, and $CoCl_2$ that quenches cytosolic fluorescence but not the mitochondrial signal (Petronilli et al. 1999). It has been demonstrated that oxidative stress induces mPTP (Du and Yan 2010), so the oxidant TBHP was added to SH-SY5Y human neuroblastoma cells to produce the opening of the pore. The cells were treated with compounds at 0.01, 0.1 and 1 μM for 10 min and 1 mM TBHP was added just before the analysis to induce the opening of mPTP. A drop of 27.6±3.9% (p<0.05) in mitochondrial fluorescence with respect to untreated cells was observed after the addition of 1 mM TBHP. The treatment of cells with sarains 1 and 2 had no protective effects against mPTP opening (data not shown) in agreement with the previous data. Nevertheless, cells treated with sarain A at 0.1 and 1 μM showed a significant increase in fluorescence, 90.4± 9.4% (p<0.05) and 86.6± 4.6% (p<0.05) respectively, compared to cells treated with 1 mM TBHP alone. These levels of mPTP inhibition are similar to the results obtained with 0.2 μM cyclosporine A (CsA) (91.1± 6.0%; p<0.05), a known potent blocker of mPTP opening (Hansson et al. 2003) (Fig. 8a).

In view of these results, we tested if sarain A was targeting CypD, a key component of the mitochondrial pore. It has been demonstrated that the PPIase activity of CypD is involved in the opening of the mPTP (Connern and Halestrap 1994).The ability of sarain A to inhibit the PPIase activity of the enzyme was determined by monitoring the rate of hydrolysis of the peptide *N*-succinyl-Ala-Ala-Pro-Phe-*p*-nitroanilide by chymotrypsin. Chymotrypsin only hydrolyses the *trans* conformer, so the rate of isomerization by CypD can be evaluated (Fischer et al. 1984).

Sarain A inhibited the PPIase activity of CypD with an IC_{50} of 0.018 μM (95% CI: 0.008- 0.037μM). This value is in the same range as the obtained with CsA (0.008 μM; 95% CI: 0.004 -0.016 μM)(Fig. 8b), which matches with previous studies with CsA and CypD(Gregory et al. 2011).

4. Discussion

The increase in life expectancy has augmented the prevalence of neurodegenerative diseases worldwide. Until now, the antioxidant compounds tested in the treatment of neurodegeneration have shown disappointing results, probably because they were focused only in one aspect of the diseases. Neurodegenerative disorders are complex and multifactorial, so the development of multitargeted drugs is considered a promising strategy to attenuate the symptoms of these conditions(Di Domenico et al.

392 2015). Particularly, the design of mitochondria-targeted antioxidants is as potential therapeutic tool for
393 the treatment of these pathologies (Moreira et al. 2010). In fact, some mitochondrial-targeted
394 antioxidants, as creatine and mitoQ, are currently in Phase I or II clinical trials(Kumar and Singh 2015).
395 In this study, the natural sponge alkaloids sarain 1, 2 and A were evaluated in an *in vitro* oxidative stress
396 model with SH-SY5Y cells to mimic oxidative damage in human brain. Sarain A was the most
397 promising compound, showing protective effects against H_2O_2-induced cell death. It also recovered
398 mitochondrial membrane depolarization and reduced ROS levels in neuroblastoma cells. These effects
399 are higher at the lower concentrations tested (0.01 and 0.1 μM). The treatment with H_2O_2 and 10 μM
400 sarain A seems to affect to the mitochondrial function, as the mitochondrial membrane is hyperpolaryzed
401 and the cell viability is decreased.
402 The antioxidant ability observed only in sarain A can be related with the differences in the structures of
403 the molecules. It has been hypothesized that the higher activity of sarain A can result from the presence
404 of a masked aldehyde group, which is known to react with the amine groups of proteins (Defant et al.
405 2011). Our results agree with previous biological studies with sarains 1, 2 and A, in which sarain A
406 showed higher antibacterial and antitumoral activity (Caprioli et al. 1992; Defant et al. 2011).
407 Mitochondrial alterations play a central role in neurodegeneration, each neurodegenerative disease
408 affects different brain areas, but all of them share mitochondrial dysfunctions (Yan et al. 2013). This
409 dysfunction is produced by several causes, as the disruption of the respiratory chain that leads to a
410 decrease in ATP levels, the impaired activity of the glucose metabolism, the opening of the mPTP or
411 the mutations in the mitochondrial DNA that can lead to the synthesis of abnormal proteins (Lee 2016;
412 Wang et al. 2014). In this sense, Nrf2 activation has been largely considered a target for
413 neurodegeneration because of its capacity to induce the expression of antioxidant enzymes (Calkins et
414 al. 2009). Recently, it has been demonstrated that Nrf2 translocation is also implicated in other
415 mechanisms that can reduce mitochondrial dysfunction. Nrf2 regulates the expression of genes related
416 to glucose metabolism (Singh et al. 2013) and can prevent oxidative thiol modifications of proteins
417 implicated in these pathways, as glyceraldehyde-3-phosphate dehydrogenase, a glycolytic enzyme
418 which oxidation can promote cell death in AD brains (Butterfield et al. 2010). Moreover, the nuclear
419 factor enhances ATP production and $\Delta\Psi_m$ by increasing the substrate availability for oxidative

420 phosphorylation (Holmstrom et al. 2013). Therefore, together with the induction of antioxidant systems,
421 Nrf2 activation implies other therapeutic targets for the treatment of the mitochondrial dysfunctions
422 observed in neurodegeneration. The treatment of human neuroblastoma cells with sarain A induces the
423 translocation of the factor to the nucleus, suggesting that the improvement observed in the mitochondrial
424 function, in the production of ATP and in the activity of SODs is related with this pathway.
425 Sarain A was also able to block the opening of mPTP by inhibiting the PPIase activity of CypD, the
426 most important initiating molecule of the mitochondrial pore. The formation of mPTP produces a sudden
427 collapse in $\Delta\Psi_m$ and the consequent disruption in the mitochondrial respiratory chain, resulting in
428 decreased ATP content and increased levels of ROS. In this sense, the improvement in mitochondrial
429 function, ATP levels and the reduction in the levels of ROS produced by the treatment with sarain A are
430 also related with the ability of the compound to block the mPTP. If the formation of mPTP is massive,
431 it produces mitochondrial swelling, the rupture of the outer mitochondrial membrane and the release of
432 pro-apoptotic proteins to the cytoplasm. The knockdown of CypD has shown promising results in AD
433 models (Du et al. 2008) and has reduced oxidative stress and ameliorated the dysfunction observed in
434 brain mitochondria (Baines et al. 2005), suggesting that the inhibition of this component of the mPTP
435 might be a potential therapeutic strategy in neurodegenerative disorders. Some examples of mPTP
436 blockers that act trough the inhibition of CypD activity are sanglifehrin A (Clarke et al. 2002) and CsA
437 (Crompton and Costi 1988). These molecules have reduced cell permeability because of their high
438 molecular weights, so its clinical applications are limited. This limitation makes necessary the
439 development of new small mPTP inhibitors (Rao et al. 2014).
440
441 **5. Conclusion**
442 Our results indicate that sarain A is the most promising compound, being able to ameliorate the
443 mitochondrial function and reduce the levels of ROS in a human neuronal model. This improvement is
444 related to the ability of the compound to induce the translocation of Nrf2 to the nucleus and with its
445 capacity to block the mPTP. As we mentioned before, these pathways are considered promising
446 therapeutic approaches for the treatment of neurodegeneration. Therefore, this compound may be a good
447 candidate for further studies in neurodegenerative disorders as AD, PD or ALS.

448 **Conflict of Interest**

449 The authors declare that they have no conflict of interest.

450

451 **References**

452 Baines CP et al. (2005) Loss of cyclophilin D reveals a critical role for mitochondrial permeability
453 transition in cell death Nature 434:658-662 doi:10.1038/nature03434

454 Blanquer-Rossello MD, Hernandez-Lopez R, Roca P, Oliver J, Valle A (2017) Resveratrol induces
455 mitochondrial respiration and apoptosis in SW620 colon cancer cells Biochim Biophys Acta
456 1861:431-440 doi:10.1016/j.bbagen.2016.10.009

457 Blihoghe D, Manzo E, Villela A, Cutignano A, Picariello G, Faimali M, Fontana A (2011) Evaluation
458 of the antifouling properties of 3-alyklpyridine compounds Biofouling 27:99-109
459 doi:10.1080/08927014.2010.542587

460 Burchell VS, Gandhi S, Deas E, Wood NW, Abramov AY, Plun-Favreau H (2010) Targeting
461 mitochondrial dysfunction in neurodegenerative disease: Part I Expert Opin Ther Targets
462 14:369-385 doi:10.1517/14728221003652489

463 Butterfield DA, Hardas SS, Lange ML (2010) Oxidatively modified glyceraldehyde-3-phosphate
464 dehydrogenase (GAPDH) and Alzheimer's disease: many pathways to neurodegeneration J
465 Alzheimers Dis 20:369-393 doi:10.3233/jad-2010-1375

466 Calkins MJ et al. (2009) The Nrf2/ARE pathway as a potential therapeutic target in neurodegenerative
467 disease Antioxid Redox Signal 11:497-508 doi:10.1089/ARS.2008.2242

468 Caprioli V, Cimino G, De Giulio A, Madaio A, Scognamiglio G, Trivellone E (1992) Selected biological
469 activities of saraines Comp Biochem Physiol B 103:293-296

470 Cardoso S, Seica RM, Moreira PI (2016) Mitochondria as a target for neuroprotection: implications for
471 Alzheimer s disease Expert Rev Neurother:1-15 doi:10.1080/14737175.2016.1205488

472 Chakraborty TR, Cohen J, Yohanan D, Alicea E, Weeks BS, Chakraborty S (2016) Estrogen is
473 neuroprotective against hypoglycemic injury in murine N38 hypothalamic cells Mol Med Rep
474 14:5677-5684 doi:10.3892/mmr.2016.5952

475 Cimino G, Mattia CA, Mazzarella L, Putili R, Scognamiglio G, Spinella A, Trivellone E (1989)
476 Unprecedented alkaloid skeleton from the mediterranean sponge reniera sarai: X-ray structure
477 of an acetate derivative of sarain-a 45:3863–3872 doi:10.1016/S0040-4020(01)89245-0

478 Cimino G, Stefano SD, Scognamiglio G, Sodano G, Trivellone E (1986) Sarains: A New Class of
479 Alkaloids from the Marine Sponge Reniera Sarai Bulletin des Sociétés Chimiques Belges
480 95:783-800 doi:10.1002/bscb.19860950907

Clarke SJ, McStay GP, Halestrap AP (2002) Sanglifehrin A acts as a potent inhibitor of the mitochondrial permeability transition and reperfusion injury of the heart by binding to cyclophilin-D at a different site from cyclosporin A J Biol Chem 277:34793-34799 doi:10.1074/jbc.M202191200

Coccini T, Manzo L, Bellotti V, De Simone U (2014) Assessment of cellular responses after short- and long-term exposure to silver nanoparticles in human neuroblastoma (SH-SY5Y) and astrocytoma (D384) cells ScientificWorldJournal 2014:259765 doi:10.1155/2014/259765

Connern CP, Halestrap AP (1994) Recruitment of mitochondrial cyclophilin to the mitochondrial inner membrane under conditions of oxidative stress that enhance the opening of a calcium-sensitive non-specific channel Biochem J 302 (Pt 2):321-324

Corona JC, Duchen MR (2015) Impaired mitochondrial homeostasis and neurodegeneration: towards new therapeutic targets? In: J Bioenerg Biomembr, vol 47. vol 1-2. pp 89-99. doi:10.1007/s10863-014-9576-6

Crompton M, Costi A (1988) Kinetic evidence for a heart mitochondrial pore activated by Ca2+, inorganic phosphate and oxidative stress. A potential mechanism for mitochondrial dysfunction during cellular Ca2+ overload Eur J Biochem 178:489-501

Defant A, Mancini I, Raspor L, Guella G, Turk T, Sepčić K (2011) New Structural Insights into Saraines A, B, and C, Macrocyclic Alkaloids from the Mediterranean Sponge Reniera (Haliclona) sarai European Journal of Organic Chemistry 2011:3761-3767 doi:10.1002/ejoc.201100434

Di Domenico F, Barone E, Perluigi M, Butterfield DA (2015) Strategy to reduce free radical species in Alzheimer's disease: an update of selected antioxidants Expert Rev Neurother 15:19-40 doi:10.1586/14737175.2015.955853

Du H et al. (2008) Cyclophilin D deficiency attenuates mitochondrial and neuronal perturbation and ameliorates learning and memory in Alzheimer's disease Nat Med 14:1097-1105 doi:10.1038/nm.1868

Du H, Yan SS (2010) Mitochondrial permeability transition pore in Alzheimer's disease: cyclophilin D and amyloid beta Biochim Biophys Acta 1802:198-204 doi:10.1016/j.bbadis.2009.07.005

Eliseev RA, Filippov G, Velos J, VanWinkle B, Goldman A, Rosier RN, Gunter TE (2007) Role of cyclophilin D in the resistance of brain mitochondria to the permeability transition Neurobiol Aging 28:1532-1542 doi:10.1016/j.neurobiolaging.2006.06.022

Esteras N, Dinkova-Kostova AT, Abramov AY (2016) Nrf2 activation in the treatment of neurodegenerative diseases: a focus on its role in mitochondrial bioenergetics and function Biol Chem 397:383-400 doi:10.1515/hsz-2015-0295

Fischer G, Bang H, Berger E, Schellenberger A (1984) Conformational specificity of chymotrypsin toward proline-containing substrates Biochim Biophys Acta 791:87-97

Gandhi S, Abramov AY (2012) Mechanism of oxidative stress in neurodegeneration Oxid Med Cell Longev 2012:428010 doi:10.1155/2012/428010

518 Gregory MA et al. (2011) Preclinical characterization of naturally occurring polyketide cyclophilin
519 inhibitors from the sanglifehrin family Antimicrob Agents Chemother 55:1975-1981
520 doi:10.1128/aac.01627-10
521 Grosso C, Valentão P, Ferreres F, Andrade PB (2014) Bioactive marine drugs and marine biomaterials
522 for brain diseases Mar Drugs 12:2539-2589 doi:10.3390/md12052539
523 Halliwell B, Whiteman M (2004) Measuring reactive species and oxidative damage in vivo and in cell
524 culture: how should you do it and what do the results mean? Br J Pharmacol 142:231-255
525 doi:10.1038/sj.bjp.0705776
526 Hansson MJ, Persson T, Friberg H, Keep MF, Rees A, Wieloch T, Elmer E (2003) Powerful cyclosporin
527 inhibition of calcium-induced permeability transition in brain mitochondria Brain Res 960:99-
528 111
529 Holmstrom KM et al. (2013) Nrf2 impacts cellular bioenergetics by controlling substrate availability for
530 mitochondrial respiration Biol Open 2:761-770 doi:10.1242/bio.20134853
531 Huang SL, He HB, Zou K, Bai CH, Xue YH, Wang JZ, Chen JF (2014) Protective effect of tomatine
532 against hydrogen peroxide-induced neurotoxicity in neuroblastoma (SH-SY5Y) cells J Pharm
533 Pharmacol 66:844-854 doi:10.1111/jphp.12205
534 Itoh K, Ye P, Matsumiya T, Tanji K, Ozaki T (2015) Emerging functional cross-talk between the Keap1-
535 Nrf2 system and mitochondria J Clin Biochem Nutr 56:91-97 doi:10.3164/jcbn.14-134
536 Kharroubi W, Nury T, Ahmed SH, Andreoletti P, Sakly R, Hammami M, Lizard G (2017) Induction by
537 arsenate of cell-type-specific cytotoxic effects in nerve and hepatoma cells Hum Exp
538 Toxicol:960327116687893 doi:10.1177/0960327116687893
539 Kumar A, Singh A (2015) A review on mitochondrial restorative mechanism of antioxidants in
540 Alzheimer's disease and other neurological conditions Front Pharmacol 6:206
541 doi:10.3389/fphar.2015.00206
542 Lee J (2016) Mitochondrial drug targets in neurodegenerative diseases Bioorg Med Chem Lett 26:714-
543 720 doi:10.1016/j.bmcl.2015.11.032
544 Leirós M et al. (2015) Gracilins: Spongionella-derived promising compounds for Alzheimer disease
545 Neuropharmacology 93:285-293 doi:10.1016/j.neuropharm.2015.02.015
546 Lin MT, Beal MF (2006) Mitochondrial dysfunction and oxidative stress in neurodegenerative diseases
547 Nature 443:787-795 doi:10.1038/nature05292
548 Lu MC, Ji JA, Jiang ZY, You QD (2016) The Keap1-Nrf2-ARE Pathway As a Potential Preventive and
549 Therapeutic Target: An Update Med Res Rev 36:924-963 doi:10.1002/med.21396
550 Magesh S, Chen Y, Hu L (2012) Small molecule modulators of Keap1-Nrf2-ARE pathway as potential
551 preventive and therapeutic agents Med Res Rev 32:687-726 doi:10.1002/med.21257
552 Malhotra D et al. (2010) Global mapping of binding sites for Nrf2 identifies novel targets in cell survival
553 response through ChIP-Seq profiling and network analysis Nucleic Acids Res 38:5718-5734
554 doi:10.1093/nar/gkq212

555 McBean GJ, Lopez MG, Wallner FK (2016) Redox-based therapeutics in neurodegenerative disease Br
556 J Pharmacol doi:10.1111/bph.13551
557 Moreira PI et al. (2010) Mitochondria: a therapeutic target in neurodegeneration Biochim Biophys Acta
558 1802:212-220 doi:10.1016/j.bbadis.2009.10.007
559 Mosmann T (1983) Rapid colorimetric assay for cellular growth and survival: application to
560 proliferation and cytotoxicity assays J Immunol Methods 65:55-63
561 Nguyen TT, Stevens MV, Kohr M, Steenbergen C, Sack MN, Murphy E (2011) Cysteine 203 of
562 cyclophilin D is critical for cyclophilin D activation of the mitochondrial permeability transition
563 pore J Biol Chem 286:40184-40192 doi:10.1074/jbc.M111.243469
564 Ouazia D, Levros LC, Jr., Rassart E, Desrosiers RR (2014) Dopamine down-regulation of protein L-
565 isoaspartyl methyltransferase is dependent on reactive oxygen species in SH-SY5Y cells
566 Neuroscience 267:263-276 doi:10.1016/j.neuroscience.2014.03.001
567 Park SY, Kim DY, Kang JK, Park G, Choi YW (2014) Involvement of activation of the Nrf2/ARE
568 pathway in protection against 6-OHDA-induced SH-SY5Y cell death by alpha-iso-cubebenol
569 Neurotoxicology 44:160-168 doi:10.1016/j.neuro.2014.06.011
570 Pertega-Gomes N et al. (2015) A glycolytic phenotype is associated with prostate cancer progression
571 and aggressiveness: a role for monocarboxylate transporters as metabolic targets for therapy J
572 Pathol 236:517-530 doi:10.1002/path.4547
573 Petronilli V, Miotto G, Canton M, Brini M, Colonna R, Bernardi P, Di Lisa F (1999) Transient and long-
574 lasting openings of the mitochondrial permeability transition pore can be monitored directly in
575 intact cells by changes in mitochondrial calcein fluorescence Biophys J 76:725-734
576 doi:10.1016/s0006-3495(99)77239-5
577 Ramsey CP et al. (2007) Expression of Nrf2 in neurodegenerative diseases J Neuropathol Exp Neurol
578 66:75-85 doi:10.1097/nen.0b013e31802d6da9
579 Rao VK, Carlson EA, Yan SS (2014) Mitochondrial permeability transition pore is a potential drug
580 target for neurodegeneration Biochim Biophys Acta 1842:1267-1272
581 doi:10.1016/j.bbadis.2013.09.003
582 Sasaki S, Tozawa T, Van Wagoner RM, Ireland CM, Harper MK, Satoh T (2011) Strongylophorine-8,
583 a pro-electrophilic compound from the marine sponge Petrosia (Strongylophora) corticata,
584 provides neuroprotection through Nrf2/ARE pathway Biochem Biophys Res Commun 415:6-
585 10 doi:10.1016/j.bbrc.2011.09.114
586 Singh A et al. (2013) Transcription factor NRF2 regulates miR-1 and miR-206 to drive tumorigenesis J
587 Clin Invest 123:2921-2934 doi:10.1172/jci66353
588 Tricarico PM, de Oliveira Franca RF, Pacor S, Ceglia V, Crovella S, Celsi F (2016) HIV Protease
589 Inhibitors Apoptotic Effect in SH-SY5Y Neuronal Cell Line Cell Physiol Biochem 39:1463-
590 1470 doi:10.1159/000447849

591 Vega-Avila E, Pugsley MK (2011) An overview of colorimetric assay methods used to assess survival
592 or proliferation of mammalian cells Proc West Pharmacol Soc 54:10-14
593 Wang X, Wang W, Li L, Perry G, Lee HG, Zhu X (2014) Oxidative stress and mitochondrial dysfunction
594 in Alzheimer's disease Biochim Biophys Acta 1842:1240-1247
595 doi:10.1016/j.bbadis.2013.10.015
596 Weidinger A, Kozlov AV (2015) Biological Activities of Reactive Oxygen and Nitrogen Species:
597 Oxidative Stress versus Signal Transduction Biomolecules 5:472-484
598 doi:10.3390/biom5020472
599 Yan MH, Wang X, Zhu X (2013) Mitochondrial defects and oxidative stress in Alzheimer disease and
600 Parkinson disease Free Radic Biol Med 62:90-101 doi:10.1016/j.freeradbiomed.2012.11.014
601 Yan W et al. (2015) Identification, synthesis and pharmacological evaluation of novel anti-EV71 agents
602 via cyclophilin A inhibition Bioorg Med Chem Lett 25:5682-5686
603 doi:10.1016/j.bmcl.2015.11.002
604 Zhang HA et al. (2012) Salvianolic acid A protects human SH-SY5Y neuroblastoma cells against
605 H(2)O(2)-induced injury by increasing stress tolerance ability Biochem Biophys Res Commun
606 421:479-483 doi:10.1016/j.bbrc.2012.04.021
607 Zhou X, Zheng W, Nagana Gowda GA, Raftery D, Donkin SS, Bequette B, Teegarden D (2016) 1,25-
608 Dihydroxyvitamin D inhibits glutamine metabolism in Harvey-ras transformed MCF10A
609 human breast epithelial cell J Steroid Biochem Mol Biol 163:147-156
610 doi:10.1016/j.jsbmb.2016.04.022

611

612

613 **Figures**

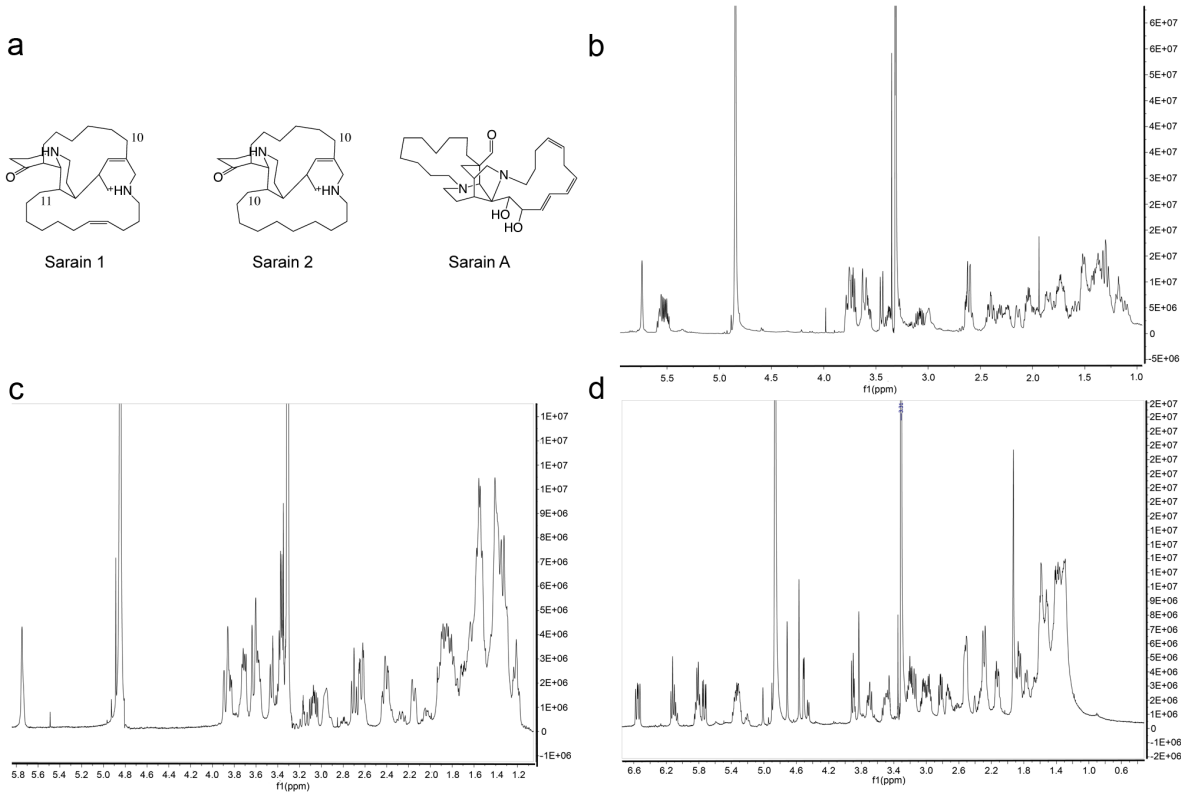

614

615 **Fig. 1** (a) Chemical structures of compounds from *Haliclona* (*Rhizoniera*) *sarai*. (b)NMR spectra of

616 sarain 1, (c) sarain 2 and (d) sarain A

617

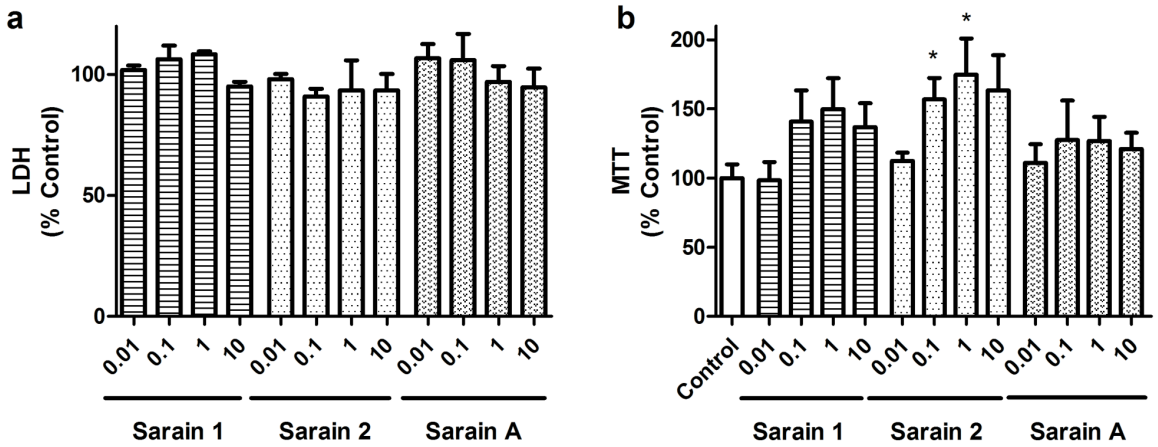

618

619 **Fig. 2** (a) Cell viability of SH-SY5Y cells treated with sarains. The cytotoxicity of the compounds at
620 0.01, 0.1, 1 and 10 µM was determined by LDH assay after 24 h of incubation. (b) Effect of sarains on
621 mitochondrial function. SH-SY5Y cells were incubated with compounds for 24 h and their effects on
622 mitochondrial function were evaluated by MTT. Values are in percentage of untreated control
623 cells.*p<0.05. Results are mean ± SEM of three independent experiments

624

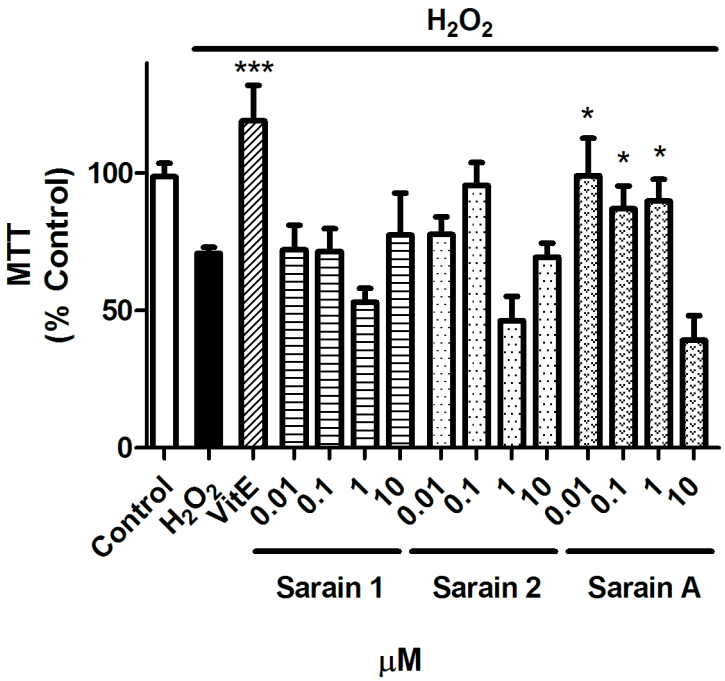

625

626 **Fig. 3** Effect of sarains on mitochondrial function against H_2O_2 insult. Mitochondrial function was
627 measured by MTT assay. SH-SY5Y cells were co-treated with 150 μM H_2O_2 and compounds at 0.01,
628 0.1, 1 and 10 μM for 6h. VitE at 25 μM was used as positive control. Sarain 1 and sarain 2 showed no
629 protective effect against H_2O_2-induced cytotoxicity. Sarain A increased cell viability at 0.01, 0.1 and 1
630 μM. The values are presented in percentage of non-treated control cells and compared to cells treated
631 with 150 μM H_2O_2 alone.*p<0.05 and ***p<0.001. Data are mean ± SEM of three or more independent
632 experiments performed by triplicate

633

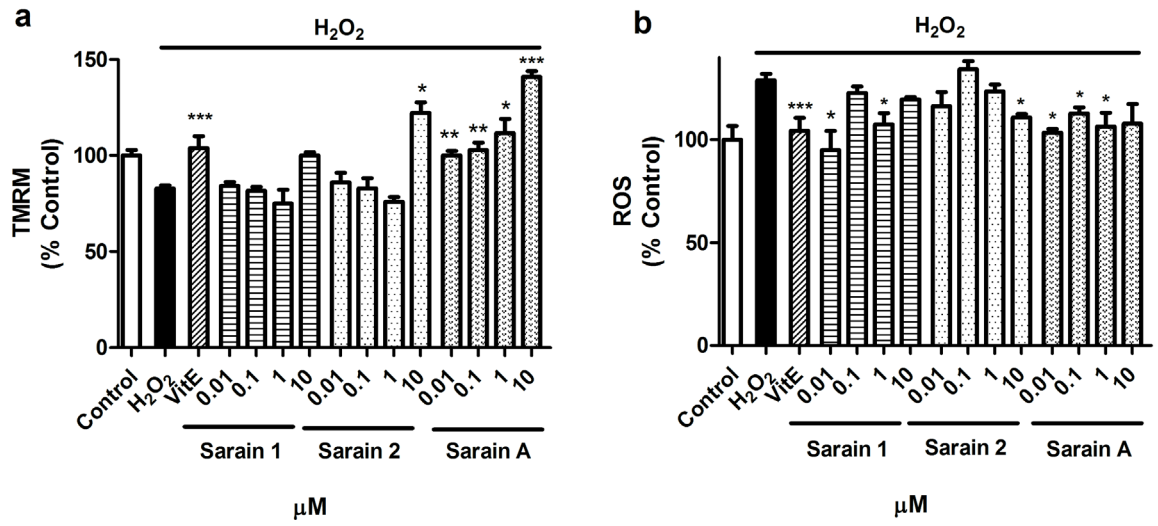

634

635 **Fig. 4** Effect of sarains on $\Delta\Psi_m$ and ROS levels. Cells were co-incubated with 150 μM H_2O_2 and sarains
636 at 0.01, 0.1, 1 and 10 μM for 6 h. 25 μM vitE was used as positive control. (a) TMRM assay was used
637 to determine the $\Delta\Psi_m$. The treatment with sarain 1 had no effect on $\Delta\Psi_m$, and sarain 2 only increased
638 $\Delta\Psi_m$ at 10 μM. Sarain A restored $\Delta\Psi_m$ levels at all the concentrations. (b) ROS levels were assessed
639 with carboxy-H_2DCFDA. Sarain 1 decreased ROS at 0.01 and 1 μM and sarain 2 diminished ROS levels
640 at 10 μM. Sarain A showed inhibition of ROS production at 0.01, 0.1 and 1 μM. Data are expressed as
641 percentage of untreated control cells and compared to cells treated only with 150 μM H_2O_2 by Student´s
642 *t* test. **p*<0.05, ***p*<0.01, ****p*<0.001. Values are mean ± SEM of three or more independent
643 experiments performed by triplicate

644

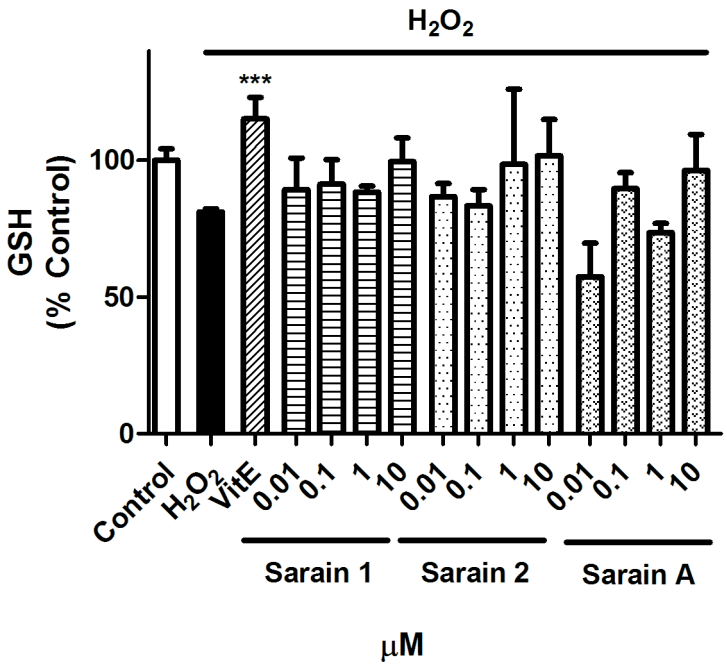

Fig. 5 Evaluation of GSH content in cells. GSH levels were measured by Thiol Tracker Violet in neuroblastoma cells co-treated with 150 μM H_2O_2 and sarains at 0.01, 0.1, 1 and 10 μM during 6h. VitE (25 μM) was used to test de validity of the *in vitro* model. Neither sarain 1, sarain 2, nor sarain A increased GSH content. Values are presented as percentage of untreated control cells and compared to cells treated only with 150 μM H_2O_2 by Student´s *t* test. ***$p<0.001$. Values are mean ± SEM of three or more independent experiments performed by triplicate

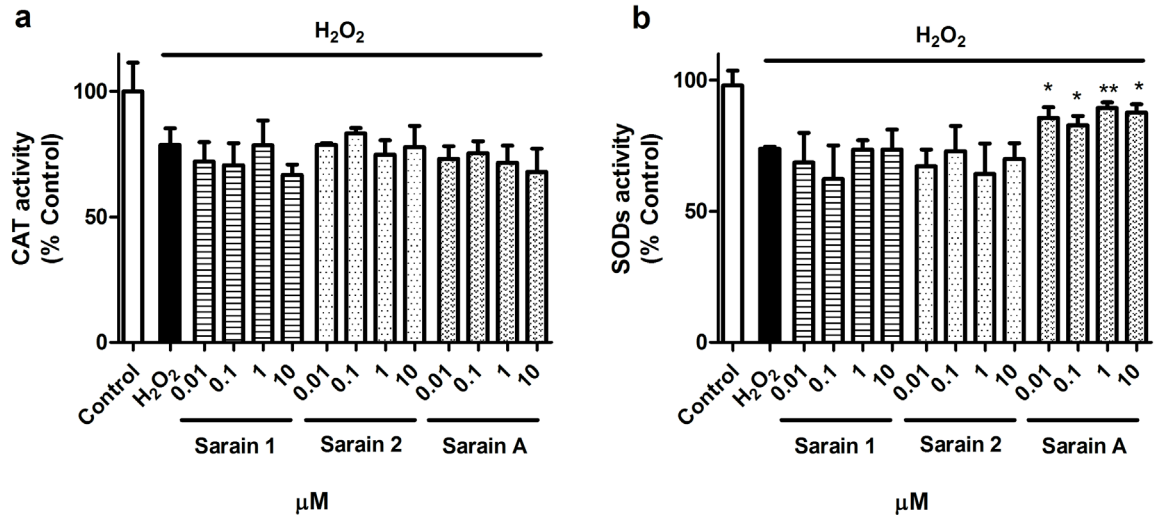

653

654 **Fig. 6** Effect of sarains on the activity of antioxidant enzymes. (a) None of the compounds increased
655 significantly the activity of CAT. (b) Sarains 1 and 2 had no effects on SODs activity, whereas sarain A
656 increased the activity of the enzymes at all the concentrations tested. Values are presented as percentage
657 of untreated control cells and compared to cells treated only with 150 μM H_2O_2 by Student´s *t* test.
658 **p*<0.05, ***p*<0.01.Values are mean ± SEM of three or more independent experiments performed by
659 triplicate

660

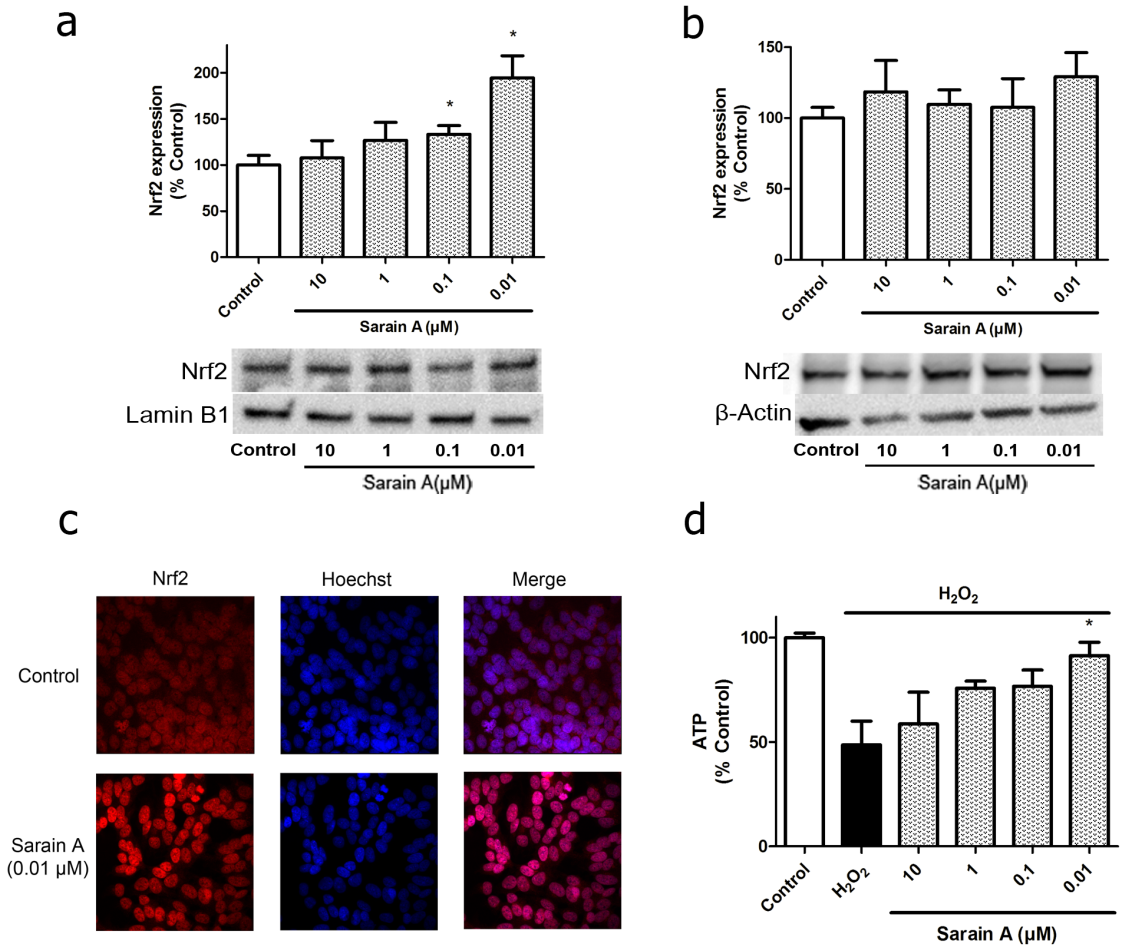

661

662 **Fig. 7** (a-c) Evaluation of Nrf2 expression. For western blot analysis (a, b), SH-SY5Y cells were
663 incubated with sarain A at 10, 1, 0.1 and 0.01 μM for 6 h. Band intensity was normalized by lamin B1
664 or β-actin in nucleus and cytosol, respectively. Values are mean ± SEM of at least three independent
665 experiments performed in duplicate and compared to control cells by Student´s *t* test. (**p*<0.05). (c)
666 Cells were treated with sarain A for 6h and immunostained with anti-Nrf2 antibody to detect the
667 localization of the transcription factor. (d) Effect of sarain A on ATP levels. Cells were co-treated with
668 the compound and 150 μM H_2O_2 for 6 h. Data are presented as percentage of untreated cells and
669 compared with cells treated with H_2O_2 alone by Student´s *t* test. (**p*<0.05)

670

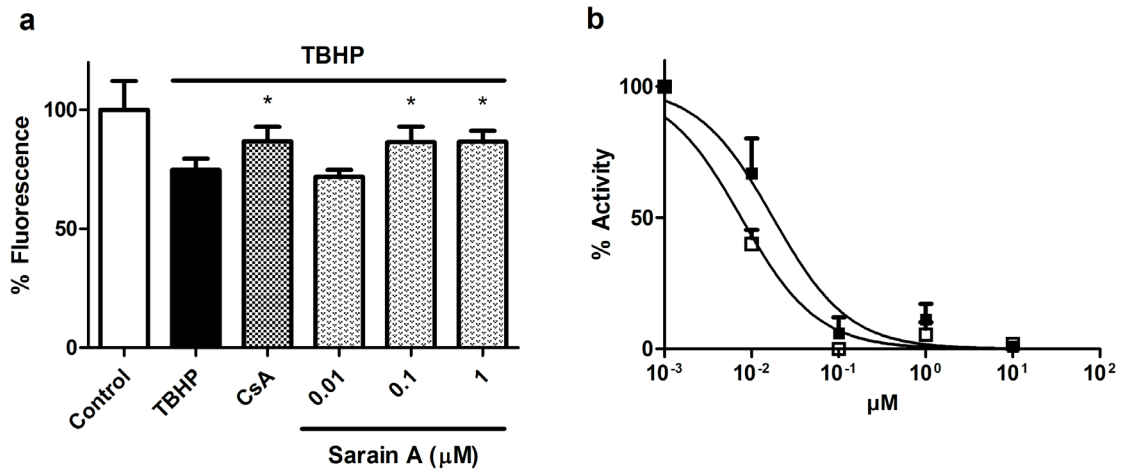

671

672 **Fig. 8** Effect of sarain A on the blockage of mPTP. (a) The extent of mPTP opening was determined by
673 flow cytometry. SH-SY5Y cells were co-treated with 1 mM TBHP and sarain A at 0.01, 0.1 and 1 μM.
674 Treatment with sarain A at 0.1 and 1 μM significantly increased the fluorescence with respect to cells
675 treated only with 1 mM TBHP. CsA at 0.2 μM also decreased mPTP opening significantly. Values are
676 presented as percentage of untreated control cells and compared to cells treated only with 1 mM TBHP
677 by Student´s *t* test. (**p*<0.05). Values are mean ± SEM of three independent experiments. (b) Inhibition
678 of CypD PPIase activity. The enzyme was incubated with sarain A (■) and CsA (□) at different
679 concentrations (0.001- 10 μM).Data are presented as percentage of the maximal PPIase activity. Values
680 are mean ± SEM of three independent experiments